



Improvement of Tightening Reliability of Bolted Joints Using Elliptical Confidence Limit in Calibrated Wrench Method

Soichi Hareyama, Ken-ichi Manabe, and Satoshi Kobayashi Tokyo Metropolitan University

Citation: Hareyama, S., Manabe, K.-i., and Kobayashi, S., "Improvement of Tightening Reliability of Bolted Joints Using Elliptical Confidence Limit in Calibrated Wrench Method," SAE Technical Paper 2020-01-0218, 2020, doi:10.4271/2020-01-0218.

Abstract

The calibrated wrench method is used in the tightening of bolts in manufacturing industries in the case of a large amount of tightening work. It is important to apply a large initial clamping force to ensure tightening reliability and prevent self-loosening, fatigue breakage, and so forth. In this method, the clamping force of bolted joints is controlled using a torque wrench. However, since the clamping force is indirectly applied by a wrench, it varies greatly in the case of a large amount of tightening in a factory. Therefore, the calibrated wrench method is not so accurate from the viewpoint of clamping force control. It is conventionally thought that the distribution of the clamping force has the shape of a rhombus. When tightening torque and clamping

force are considered to be two independent random variables, the clamping force is distributed within an elliptical confidence limit. Here, we show that the distribution of equivalent stress also has an elliptical confidence limit. Considering the permitted limit for working load stress on a bolted joint, the elliptical distribution has a larger margin to the yield point than the conventional rhombic distribution. Using this feature, we can set a higher target tightening torque than before. We show that a higher tightening torque and initial clamping force can be obtained with smaller variation than before. Finally, we establish a method for maintaining the tightening reliability that involves applying a large clamping force by increasing the target tightening torque using the elliptical confidence limit.

Introduction

Screw threads and bolted joints play an important role in many industrial products such as cars, construction equipment, industrial machines, railroad vehicles, bridges, electrical machinery, hydraulic equipment, airplanes, infrastructure, and plant equipment. Although screws and bolts are machine parts based on a simple principle involving a wedge and a spiral and have been in use for more than 2000 years, problems such as poor bolting, self-loosening, and insufficient strength occur even today. Why do problems with screw threads still occur? Why do they continue to be a machine element requiring special attention? The basic issues associated with bolted joints are listed in [Table 1](#).

The turn-of-nut method, torque gradient control method, and plastic-region tightening are examples of methods developed to obtain a large initial clamping force (axial tension) with sufficient accuracy. However, the calibrated wrench method is still widely used because of the simple tool and easy standardization.

The optimum condition of tightening bolted joints used in a machine is defined as the state in which the joints are tightened with a sufficiently high clamping force to be free from breakage and loosening by any external force during machine operation [1, 2, 3, 4]. We previously proposed methods of load analysis and lifetime evaluation of fatigue failure in bolted

joints [5]. We conducted a fundamental observation and analysis of the loosening phenomenon and also measurements and analysis of the loosening of bolted joints of components and industrial machines [6].

Many studies have been conducted on tightening reliability. For example, Bickford [7] described the theory of tightening and introduced one of the equations relating the tightening torque and preload. He also showed the variation of the nut factor (torque coefficient). In recent research, Nassar and Yang [8] theoretically investigated the torque-tension relationship in terms of the coefficient of friction. Amir et al. [9] predicted the failure of bolted joints using von Mises stress. Kopfer et al. [10] derived torque and preload equations and the coefficient of friction at the thread.

Bolt tightening and slope dynamics are intimately related. As shown by the dot-dashed line in [Figure 1](#), when tightening a bolt using a torque wrench or the like, the clamping force of the bolt also increases when a tightening torque is applied. When tightening is completed with the target tightening torque (red circle in the figure) and the torque wrench is removed, the initial clamping force (red arrow in the figure) is obtained. A large number of tightening operations are performed on a production line of a factory, where the initial clamping force varies greatly. Conventionally, this kind of distribution has been assumed to have a rhombic shape, as

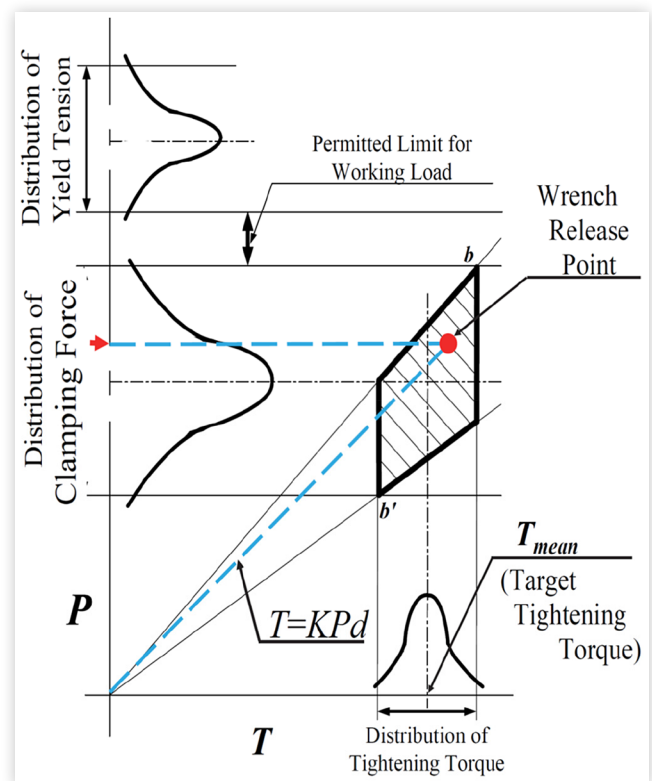
TABLE 1 Basic issues associated with bolted joints

Issues	Details
1. How to maintain tightening reliability	<ol style="list-style-type: none"> 1. High initial clamping force is required, therefore plastic tightening methods have been developed. However, applying a high initial clamping force is not straightforward, and even today a calibrated wrench method must be used in many cases. 2. Turn-of-nut method, torque gradient control method, plastic-region tightening, etc., are improved methods of obtaining a high initial clamping force. 3. Breakage of screw threads and damage through deformation (cross-sectional reduction) may be caused by tightening. 4. Establish a clamping force for tightening reliability.
2. How to analyze and measure load on bolted joints	<ol style="list-style-type: none"> 1. An axial force, bending moment, or torsional torque is often applied to bolted joints. 2. How to measure and obtain the load on bolted joints. 3. Establish a load analysis method. 4. How to feed back the load measurement and analysis results to design and experimental stages.
3. How to prevent self-loosening and failure	<ol style="list-style-type: none"> 1. Self-loosening easily occurs owing to the spiral shape and is affected by the depression of the bearing surface. 2. Fundamental study of the self-loosening phenomenon is very important. 3. Establish a method for predicting lifetime to loosening failure and residual clamping force (axial tension) estimation. 4. Establish a method for design based on judgement criteria for self-loosening.
4. How to prevent breakage (Fatigue breakage, etc.)	<ol style="list-style-type: none"> 1. Bolted joints are often under high stress and subjected to a vibrational force and repeated external forces. 2. Areas of high stress concentration exist in the underhead fillet part and threaded portion. 3. As a result, fatigue breakage and hydrogen embrittlement may occur during machine operation. 4. Establish a method for predicting lifetime to fatigue failure and embrittlement failure. 5. Establish a method for design based on judgement criteria for infinite lifetime design and finite lifetime design.
5. Other issues	<ol style="list-style-type: none"> 1. There are also many types of bolt and screw (coarse/fine screw threads with different strengths and electroplated coatings). 2. Many bolted joints are used in a single product. 3. Suitable maintenance is required to maintain the initial performance of bolted joints and long-term safety.

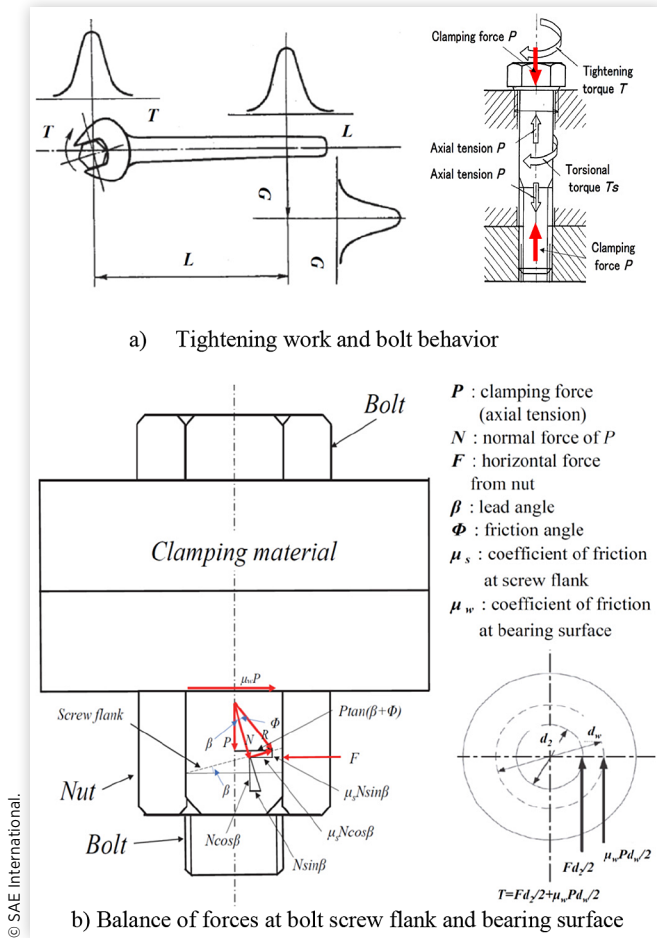
© SAE International.

shown by the hatched area in [Figure 1](#). This is due to variations in the tightening torque and torque coefficient (nut factor). The tightening torque is obtained as the product of the distance L to the action point and the force G as shown in [Figure 2-a](#). We also show schematically the bolt behavior and the balance of forces at the bolt screw flank and bearing surface in [Figure 2-b](#)). The basic formula of the calibrated wrench method can be derived from the balance of forces in the horizontal and vertical directions. Details are given in the next section ([Equations \(1\) to \(4\)](#)).

The tightening torque depends on the management status of the tool and the work posture of the operator. On the other hand, the torque coefficient depends on the friction coefficients of the thread surface and bearing surface, which in turn depend on the lubrication conditions and the properties of the screw. The cause of the variations in the tightening torque and torque coefficient is irrelevant, and when the tightening torque and torque coefficient are considered as independent random variables, their distribution has an elliptical shape as shown in [Figure 3](#). The key point of our proposed method is that this elliptical confidence limit has a narrower range than the conventional rhombic distribution. This concept can be applied to not only the relationship between the tightening torque and the clamping force (axial tension or axial stress) but also the relationship between the tightening torque and the equivalent stress shown in elliptical coordinates in [Figure 3](#). Details will be given in the following.

FIGURE 1 Relation between tightening torque and clamping force (conventional method)

© SAE International.

FIGURE 2 Tightening work by wrench and behavior of bolt

$$\text{where } \tan \beta = p / (\pi d_2). \quad (4)$$

Here, d is the nominal diameter, d_2 is the basic pitch diameter of the external thread, d_w is the diameter of the bearing surface equivalent to the friction torque, p is the pitch, α is half of the thread angle, β is the lead angle, Φ is the friction angle of triangular screw thread flank ($\Phi = \tan^{-1}(\mu_s \sec \alpha)$), K is the torque coefficient (nut factor), K_1 is the torque coefficient between screw flanks, K_2 is the clamping force (axial tension) torque coefficient, K_3 is the bearing surface torque coefficient, μ_s is the coefficient of friction between screw flanks, and μ_w is the coefficient of friction at the bearing surface.

The torque T_s exerted on the torsion of a bolt during tightening is expressed as

$$T_s = (K_1 + K_2) Pd = K_s Pd = \eta T. \quad (5)$$

Here, K_s is the torsion torque coefficient ($K_s = K_1 + K_2$) and η is the torsion torque ratio ($\eta = K_s / K$).

Then, the coefficients of friction are obtained as

$$\mu_s = 2d \{ T_s / (Pd) - K_2 \} / (d_2 \sec \alpha) \quad (6)$$

$$\mu_w = (2d / d_w) \{ k - T_s / (Pd) \}. \quad (7)$$

When $\mu = \mu_s = \mu_w$,

$$\mu = \frac{2Kd - d_2 \tan \beta}{d_2 \sec \alpha + d_w}. \quad (8)$$

When d_s is the diameter of the stress area and A_s is the cross section of the stress area, the axial stress of a screw thread in the stress area σ and the shear stress of a screw thread in the stress area τ are expressed as the following equations:

$$\sigma = P / A_s = T / (KA_s d) \quad (9)$$

$$\tau = \frac{16T_s}{\pi d_s^3} = \frac{16\eta T}{\pi d_s^3}. \quad (10)$$

Figure 4 shows the relationship between K and η in a metric screw thread for different μ_s , μ_w , and μ .

When the breakage of a bolted joint made of mild steel or carbon steel is explained in accordance with shear strain energy theory (the von Mises yield criterion), the equivalent stress σ_e is expressed as

$$\sigma_e = \sqrt{\sigma^2 + 3\tau^2}. \quad (11)$$

The variation in the tightening torque of a large number of bolted joints is represented by the tightening work coefficient a given by Equation (12). The coefficient a depends not only on the tightening tool accuracy but also on the management state, the work posture, and the process control capability of the tool or shop floor at a production site. Bickford [11] has summarized the grade of variation for every tightening tool and work method.

According to his classification, a variation of about 3-15% ($a=0.03-0.15$) is sufficient for the tightening work coefficient a in the calibrated wrench method. He indicated that the tightening accuracy can be $\pm 20\%$ ($a=0.2$) when the accuracy is low. Regarding how to control the quality of screw thread tightening in the production process, Kawasaki et al. [12] analyzed the concept of classifying the error (variation) for

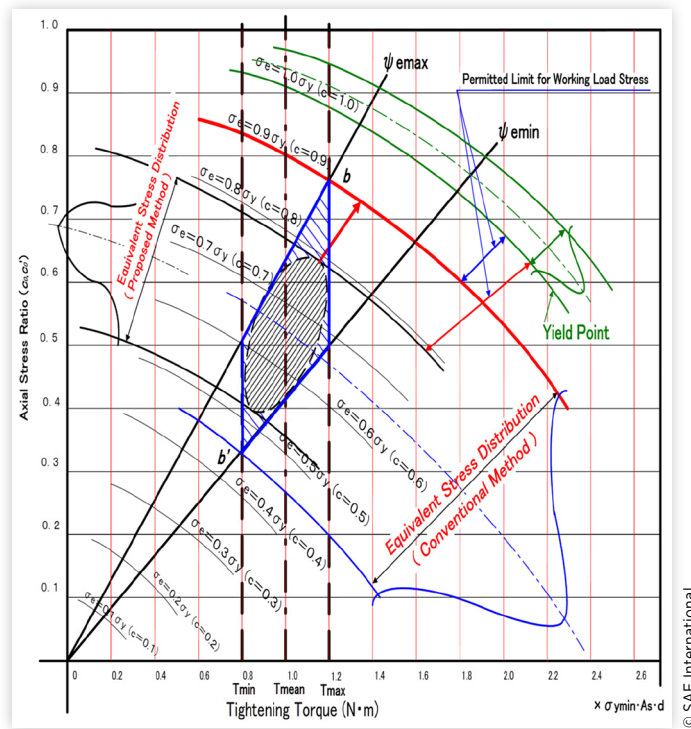
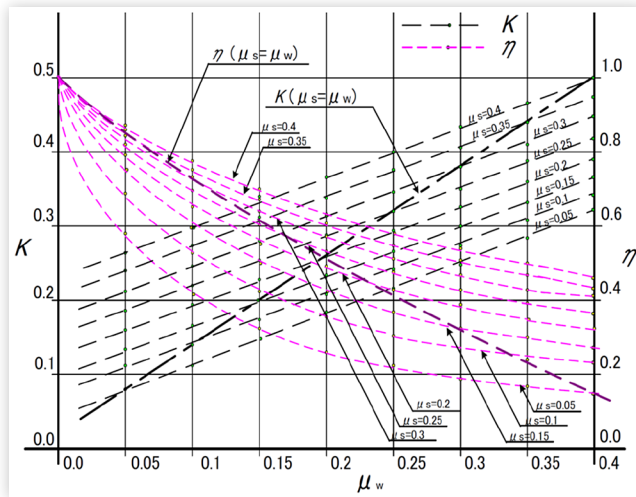
Principle of Bolted Joint Tightening by Calibrated Wrench Method (Conventional View)

Generally, for the examples referred to in our previous papers [2, 3] and by Nassar and Yang [8], as shown by the dot-dashed line in Figures 1 and 2, the relationship between the tightening torque T and the clamping force (axial tension) P for a triangular screw thread is theoretically expressed as

$$\begin{aligned} T &= KPd = (K_1 + K_2 + K_3)Pd \\ &= \{d_2 \tan \Phi + d_2 \tan \beta + d_w \mu_w\} P / 2 \\ &= \left(\mu_s d_2 \sec \alpha + \frac{p}{\pi} + d_w \mu_w \right) \frac{P}{2}. \end{aligned} \quad (1)$$

$$\begin{aligned} K &= (d_2 \mu_s \sec \alpha + d_2 \tan \beta + d_w \mu_w) / 2 \\ &= K_1 + K_2 + K_3 \end{aligned} \quad (2)$$

$$K_1 = d_2 \mu_s \sec \alpha / 2, K_2 = d_2 \tan \beta / 2, K_3 = d_w \mu_w / 2. \quad (3)$$

FIGURE 3 Relationship between tightening torque, axial stress, and equivalent stress (proposed method)**FIGURE 4** Relationship between K and η 

the tightening torque accuracy ($\pm 30\%$, $a=0.3$) of the calibrated wrench method.

The maximum and minimum tightening torques, tightening work coefficient, and tightening coefficient Q are given by the following equations:

$$a = (T_{max} - T_{min}) / (2T_{mean}) \quad (12)$$

$$T_{max} = (1 + a)T_{mean} \quad (13)$$

$$T_{min} = (1 - a)T_{mean} \quad (14)$$

$$Q = \frac{P_{max}}{P_{min}} = \frac{(1 + a)K_{max}}{(1 - a)K_{min}} \quad (15)$$

Here, T_{mean} is the target tightening torque, T_{max} is the maximum tightening torque in the distribution, T_{min} is the minimum tightening torque in the distribution, K_{max} is the maximum torque coefficient in the distribution, K_{min} is the minimum torque coefficient in the distribution, P_{max} is the maximum clamping force in the distribution, and P_{min} is the minimum clamping force in the distribution.

In the case that a structure is tightened by a bolted joint, these equations are well established as part of general tightening theory.

In many studies on tightening carried out on the production line of a factory, for example, it has been supposed that the variation in clamping force is distributed in the form of a rhombus, as shown by the hatched area in Figure 1. Point b in the figure is located at P_{max} and point b' is located at P_{min} .

On the other hand, Equation (11) can be expressed as

$$\begin{aligned} \sigma_e &= \sqrt{\sigma^2 + 3\tau^2} = \sqrt{\left(\frac{1}{K}\right)^2 + 3\left(4\eta\frac{d}{d_s}\right)^2} \frac{T}{A_s d} \\ &= \varnothing_e \frac{T}{A_s d} = \varnothing_e T' / A_s. \end{aligned} \quad (16)$$

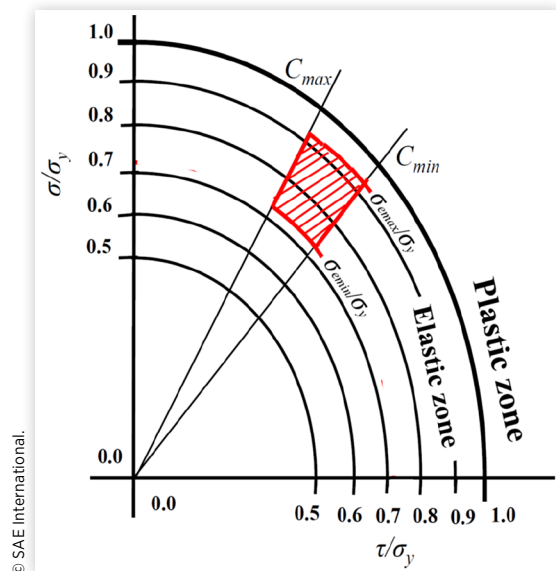
Here, \varnothing_e is the equivalent stress coefficient and T' is the unit tightening torque.

Then, the maximum equivalent stress σ_{emax} and minimum equivalent stress σ_{emin} are similarly expressed by the following equations:

$$\sigma_{emax} = \frac{(1 + a)\varnothing_{emax} T_{mean}}{A_s d} \quad (17)$$

$$\sigma_{emin} = \frac{(1 - a)\varnothing_{emin} T_{mean}}{A_s d} \quad (18)$$

FIGURE 5 Relation among σ , τ , σ_{emax} , and σ_y based on shear strain energy theory



From Equation (16), when σ_e is treated as yield point σ_y , the relationship among σ , τ , σ_{emax} , and σ_y is obtained as Equation (19), which is illustrated in Figure 5 to help provide a general understanding. Note that the figure shows only the first quadrant of the ellipse.

$$\frac{(\sigma / \sigma_y)^2}{A^2} + \frac{(\tau / \tau_y)^2}{B^2} = 1 \quad (19)$$

A and B : constants

Assuming that the hatched zone in the figure has a slope of C , the slope is expressed by the following equation:

$$C = (d_s / K)(4\eta d). \quad (20)$$

In many tightening works, C takes maximum and minimum values that depend on the torque coefficient K and the torsion torque ratio η , that is, the coefficient of friction. In Figure 5, the outer curve of the hatched area is σ_{emax}/σ_y and the inner curve of the hatched area is σ_{emin}/σ_y in elliptical coordinates.

Distribution Principle for Product of two Independent Probability Variables

Two independent probability variables are denoted by x and y , and their product z is defined as

$$z = xy. \quad (21)$$

Now, the product z is also a probability variable, and all three probability variables, x , y , and z , are assumed to have normal distributions. Accordingly, the probability density

TABLE 2 List of probability variables and functions

Variable	pdf.	Nomai distribution
x	$f(x)$	$N(\mu_x, \sigma_x^2)$
y	$g(y)$	$N(\mu_y, \sigma_y^2)$
z	$h(z)$	$N(\mu_z, \sigma_z^2)$

pdf.: probability density function

functions and normal distributions of x , y , and z are given in Table 2. When Equation (21) is rewritten using probability density functions, Equation (22) is obtained.

$$h(z) = f(x) \cdot g(y) \quad (22)$$

Since $f(x)$ and $g(y)$ are considered to be mutually independent, $h(z)$ becomes a coupling probability density function. $h(z)$ can be expressed as

$$h(z) = \frac{1}{\sqrt{2\pi}\sigma_z} \exp\left\{-\frac{1}{2} \frac{(z - \mu_z)^2}{\sigma_z^2}\right\}. \quad (23)$$

On the other hand, the right side of Equation (22) can be expressed as

$$\begin{aligned} & f(x) \cdot g(y) \\ &= \frac{1}{2\pi\sigma_x\sigma_y} \exp\left\{-\frac{1}{2} \left[\frac{(x - \mu_x)^2}{\sigma_x^2} + \frac{(y - \mu_y)^2}{\sigma_y^2} \right]\right\}. \end{aligned} \quad (24)$$

As mentioned above, since the product of $f(x)$ and $g(y)$ is a coupled probability density function and also a normal distribution, Equations (23) and (24) must be equivalent for all values of x , y , and z . Therefore, the following equations are obtained:

$$\sigma_z = \sqrt{2\pi}\sigma_x\sigma_y \quad (25)$$

$$\frac{(z - \mu_z)^2}{\sigma_z^2} = \frac{(x - \mu_x)^2}{\sigma_x^2} + \frac{(y - \mu_y)^2}{\sigma_y^2}. \quad (26)$$

Since x and y are mutually independent, for x , y , and z to satisfy Equation (26), we find that $x = \mu_x$ and $y = \mu_y$ when $z = \mu_z$. From these relations and Equation (21), we obtain

$$\mu_z = \mu_x\mu_y. \quad (27)$$

Here, the variable z is given by

$$z = \mu_z + r\sigma_z, \quad (28)$$

Here, r is the random variable of z , which serves as the standard score of a normal distribution when z is expressed in terms of μ_z and σ_z (percentile value in normal distribution).

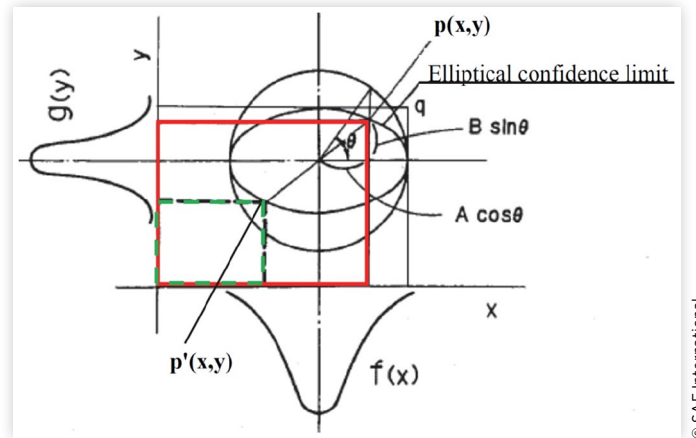
Then, Equation (26) becomes

$$\frac{(x - \mu_x)^2}{A^2} + \frac{(y - \mu_y)^2}{B^2} = 1, \quad (29)$$

where $A = r\sigma_x$

$$B = r\sigma_y.$$

This demonstrates that the confidence limit is elliptical, as shown in Figure 6. An arbitrary point on the ellipse is denoted by $p(x, y)$. Thus, z , the product of x and y from Equation (21), is given by the area enclosed by both coordinate

FIGURE 6 Elliptical confidence limit

axes and the two straight lines passing through point $p(x, y)$ parallel to them. Using the angle θ in the figure, we obtain z expressed by $Z(\theta)$ as follows:

$$Z(\theta) = (\mu_x + A \cos \theta)(\mu_y + B \sin \theta). \quad (30)$$

To determine the maximum value of $Z(\theta)$, it suffices to differentiate Equation (31) with respect to θ and determine the values of θ that give the maximum and minimum $Z(\theta)$.

$$Z'(\theta) = -A(\mu_y + B \sin \theta) \sin \theta + B(\mu_x + A \cos \theta) \cos \theta \quad (31)$$

In this case, it is clear that a point $p(x, y)$ that gives the maximum value of $Z(\theta)$ exists in the first quadrant of the ellipse in the figure. From the form of $Z(\theta)$, it is a gradually decreasing function in the range of θ from 0° to 90° and has only one solution θ_z , giving the point at which $Z(\theta)$ becomes maximum. On the other hand, $p'(x, y)$ is also the point giving the minimum value of $Z(\theta)$ with respect to the center of the ellipse; therefore, the maximum value Z_{max} and minimum value Z_{min} of $Z(\theta)$ can be expressed as follows:

$$Z_{max} = (\mu_x + A \cos \theta_z)(\mu_y + B \sin \theta_z) \quad (32)$$

$$Z_{min} = (\mu_x - A \cos \theta_z)(\mu_y - B \sin \theta_z). \quad (33)$$

Since it is assumed that z is also a normal distribution, from Equations (30) and (31), the mean value and standard deviation of $Z(\theta)$ are determined as follows:

$$\mu_z = \mu_x \mu_y + r^2 \sigma_x \sigma_y \sin \theta_z \cos \theta_z \quad (34)$$

$$\sigma_z = \mu_x \sigma_y \sin \theta_z + \mu_y \sigma_x \cos \theta_z. \quad (35)$$

Elliptical Confidence Limit of Clamping Force (Axial Tension)

When the axial tension coefficient k is expressed as

$$k = 1 / K, \quad (36)$$

then

$$P = kT / d = kT' \quad (37)$$

$$k = 2 / (d_2 \mu_s \sec \alpha + d_2 \tan \beta + d_n \mu_w) \quad (38)$$

$$\sigma = P / A_s = kT / (A_s d) = kT' / A_s. \quad (39)$$

In accordance with tightening theory, the relationship between the unit tightening torque T' and the axial tension coefficient k is expressed by Equation (39). In the equation, the variables describing the dimensions of screw threads, such as the nominal diameter d and stress area A_s , can be treated as constants when solving the equation. The coefficient k essentially becomes a function of μ_s and μ_w . On the other hand, the unit tightening torque T' is determined by the length of the torque wrench and the force it exerts. Therefore, it is permissible to consider k and T' as independent random variables.

Now, $f(T')$ has the normal distribution $N(\mu_{T'}, \sigma_{T'}^2)$ and $g(k)$ has the normal distribution $N(\mu_k, \sigma_k^2)$. Equation (29) becomes

$$\frac{(T' - \mu_{T'})^2}{A^2} + \frac{(k - \mu_k)^2}{B^2} = 1. \quad (40)$$

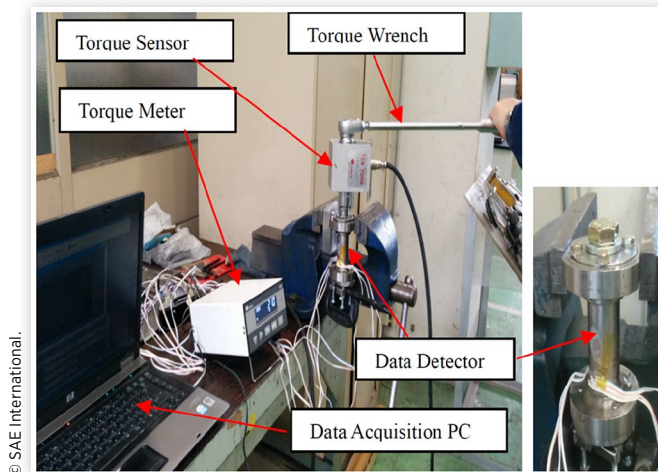
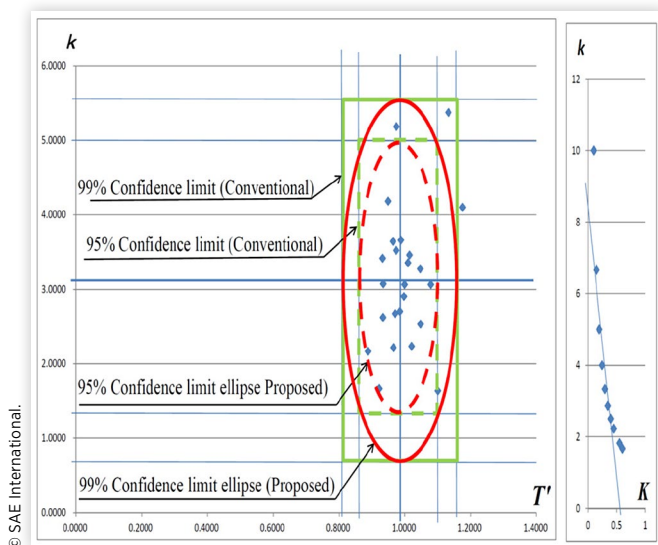
where $A = r_e \sigma_T$ and $B = r_e \sigma \mu_k$.

From Equations (30) and (31), the clamping force P and its derivative are respectively given by

$$P = (\mu_{T'} + A \cos \theta)(\mu_k + B \sin \theta) \quad (41)$$

$$P'(\theta) = -A(\mu_k + B \sin \theta) \sin \theta + B(\mu_{T'} + A \cos \theta) \cos \theta. \quad (42)$$

In accordance with our experimental study [4], we use a data detector to obtain tightening characteristics as shown in Figure 7. Figure 7 also shows the setup for the tightening test. From the test results, the initial clamping force and axial stress are found to be distributed within an elliptical confidence limit, as shown in Figure 8; note that the figure is similar to Figure 6. When the axial tension coefficient k is expressed as Equation (36), the relationship between the tightening torque and the clamping force (axial stress) is determined as Equation (37) or (39).

FIGURE 7 Setup for tightening test on bolted joints**FIGURE 8** Results for axial tension coefficient plotted within elliptical confidence limit and relationship between k and K ($K=0.1-0.6$) [4]

Normally, the torque coefficient K is approximately between 0.1 and 0.6. Thus, the relationship between k and K can be expressed by the linear equation $k = -13.67K + 8.59$ as a result of our experimental approach. Figure 8 shows the results for the axial tension coefficient, which is plotted with an elliptical confidence limit based on Equation (40). In the figure, almost all the data are plotted within the confidence limit. The validity of the elliptical confidence limit for the clamping force (axial stress) is therefore verified.

Then, the maximum and minimum clamping forces are respectively obtained as Equations (43) and (44).

$$P_{max} = \left(1 + \frac{r_p}{r_T} a \cos \theta_A \right) \times \left\{ \frac{r_K (K_{max} + K_{min}) + r_p (K_{max} - K_{min}) \sin \theta_A}{2r_K K_{max} K_{min}} \right\} \frac{T_{mean}}{d} \quad (43)$$

$$P_{min} = \left(1 - \frac{r_p}{r_T} a \cos \theta_A \right) \times \left\{ \frac{r_K (K_{max} + K_{min}) - r_p (K_{max} - K_{min}) \sin \theta_A}{2r_K K_{max} K_{min}} \right\} \frac{T_{mean}}{d} \quad (44)$$

Here, r_p and r_K are random variables of P and K , respectively, which serve as the standard scores of a normal distribution.

Elliptical Confidence Limit in Equivalent Stress

When the breakage of bolted joints is explained in accordance with shear strain energy theory, the relationship between the tightening torque and the equivalent stress σ_e is expressed by Equation (16). The coefficient ψ_e essentially becomes a function of μ_s and μ_w . It is permissible to consider ψ_e and T' as independent random variables similarly to k and T' .

Now, $f(T)$ has the normal distribution $N(\mu_T, \sigma_T^2)$ and $g(\psi_e)$ has the normal distribution $N(\mu_{\psi_e}, \sigma_{\psi_e}^2)$. If the equivalent stress σ_e has the normal distribution $N(\mu_{\sigma_e}, \sigma_{\sigma_e}^2)$, and if the equivalent stress σ_e is also expressed by the equation $\sigma_e = \mu_{\sigma_e} + r_e \sigma_{\sigma_e}$, then Equation (29) becomes

$$\frac{(T - \mu_T)^2}{A^2} + \frac{(\psi_e - \mu_{\psi_e})^2}{B^2} = 1, \quad (45)$$

where $A = r_e \sigma_T$ and $B = r_e \sigma_{\psi_e}$. r_e is the (substituted) random variable that corresponds to a cumulative percentage of a normal distribution when expressing the equivalent stress σ_e in terms of μ_{σ_e} and σ_{σ_e} (90% confidence limit $r_e = 1.645$). The elliptical confidence limit given by Equation (45) is shown in Figure 9.

From Equation (30), σ_e is given by

$$\sigma_e = (\mu_T + A \cos \theta) (\mu_{\psi_e} + B \sin \theta) / (A_s d). \quad (46)$$

Finally, the proposed maximum and minimum equivalent stresses σ_e' can be obtained from Equations (47) and (48), which are based on Equations (32) and (33), respectively.

$$\sigma'_{emax} = (1 + a \cos \theta_e) \times \left\{ (\psi_{emax} + \psi_{emin}) + (\psi_{emax} - \psi_{emin}) \sin \theta_e \right\} \frac{T_{mean}}{2A_s d} \quad (47)$$

$$\sigma'_{emin} = (1 - a \cos \theta_e) \times \left\{ (\psi_{emax} + \psi_{emin}) - (\psi_{emax} - \psi_{emin}) \sin \theta_e \right\} \frac{T_{mean}}{2A_s d} \quad (48)$$

Now, σ'_{emax} is equal to the value at $s(T, \psi_e)$ in the lower figure of Figure 9, which is lower than the value at point $q(T, \psi_e)$, at which the maximum is obtained by the conventional method. The position of $s(T, \psi_e)$ is lower than that of $q(T, \psi_e)$. Therefore, the value at point s has a margin to the yield point and can be moved up to the position of point q , as shown in the upper figure of Figure 9, when using the elliptical confidence limit.

Figure 10 shows the equivalent stress coefficient plotted as a 95% elliptical confidence limit (solid line) and a 99%

elliptical confidence limit (dashed line) obtained in the experimental study [4]. Almost all the data lie within the 95% elliptical confidence limit.

The relationship between the maximum equivalent stress σ'_{emax} and the lower limit σ_{ymin} can be expressed by Equation (49), in which c' is the true initial equivalent stress ratio.

$$\sigma'_{emax} = c'_{max} \sigma_{ymin} \quad (49)$$

The new proposed target value T'_{mean} of the tightening torque is expressed by Equation (50), which can be obtained by solving Equations (47) and (49).

$$T'_{mean} = \frac{2c'_{max} \sigma_{ymin} A_s d}{(1 + a \cos \theta_e) \left\{ \begin{array}{l} (\psi_{emax} + \psi_{emin}) \\ + (\psi_{emax} - \psi_{emin}) \sin \theta_e \end{array} \right\}} \quad (50)$$

Here, ψ_{emax} is the maximum equivalent stress coefficient in the distribution, ψ_{emin} is the minimum equivalent stress

FIGURE 9 Elliptical confidence limit for equivalent stress [2]

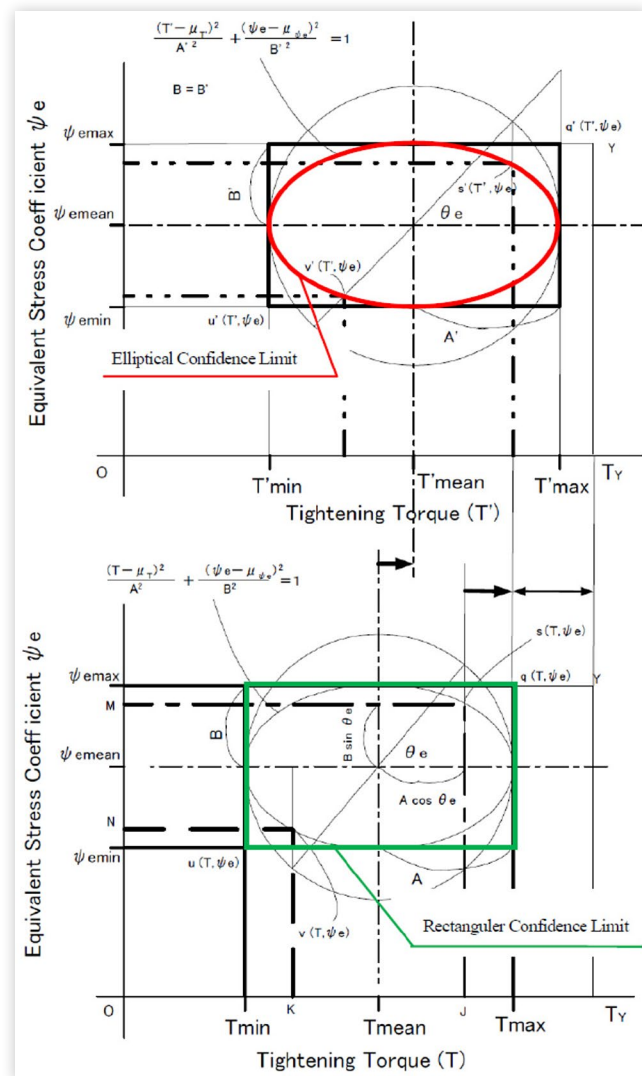
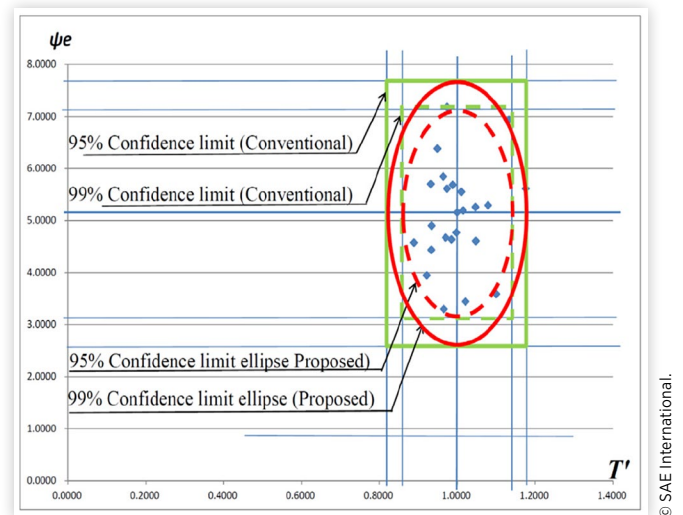


FIGURE 10 Results for equivalent stress coefficient plotted within elliptical confidence limit



coefficient in the distribution, and θ_e is the angle corresponding to the coordinates of point $s(T, \psi_e)$.

Thus, the main purpose of this figure is to show that the data are distributed in the ellipse shown in the upper panel of Figure 9 rather than the rectangle in the lower panel.

Experimental Results of Thread Characteristics

The coefficient of friction is highly variable, as also shown by the experimental results of Nassar and Yang [8]. However, it is considered that the variations in the torque coefficient K and coefficient of friction μ can be reduced by changing the lubrication condition, the limitation of the bolt to be tightened, and the limitation of the tightening tool, and by the appropriate periodic inspection and management and standardization of the operation. Table 3 shows the tightening test results for a large number of bolts [2]. In contrast to the tightening test under the dry condition, that under lubrication with machine oil shows small variations of the coefficient of friction.

TABLE 3 Experimental values for torque coefficient K , torque ratio η , coefficient of friction μ , and equivalent stress coefficient ψ_e in bolted joint tightening [3]

Lubrication Parameter	Dry		Machine Oil	
	Max	Min	Max	Min
Axial Tension Coefficient k	4.167	1.508	6.098	4.184
Torque Ratio η	0.620	0.250	0.620	0.250
Equivalent Stress Coefficient ϕ_e	6.443	2.490	7.832	4.630
Friction Coefficient $\mu (\mu_s = \mu_w)$	0.536	0.183	0.182	0.119
θ_e (Maximum Equivalent Stress)	60.7°		50.4°	
θ_p (Maximum Axial Tension)	61.2°		43.4°	

Here, θ_e is the angle corresponding to the coordinates of point $s(T, \psi_e)$ on the elliptical confidence limit giving maximum equivalent stress (see Figure 6) and θ_p is the angle giving the maximum and minimum of the axial tension distribution on the elliptical confidence limit.

Analysis of Clamping Force and Equivalent Stress Distribution of Bolted Joints

Using the results in Table 3, we investigated how the elliptical confidence limit changes with the tightening work coefficient a and the coefficient of friction μ . Figure 11 shows the change in the dispersion of the elliptical confidence limit with a . It is considered that a should be in the range from 0.2 to 0.3 in the preparation of the tightening torque standard for an entire factory or company. In each production process where the work site is fixed, a is likely to be set in the range from 0.1 to 0.2. Furthermore, in the case where lubrication, limitation of the bolts to be tightened, limitation of the tightening tools, and appropriate periodic inspection and control are performed, it is considered that a can be set in the range from 0.05 to 0.1.

From the normalized tightening torque, the tightening coefficient a was determined to be 0.122 at the 95% confidence limit and 0.161 at the 99% confidence limit of the range in the previous study [4]. It is shown that the area of the elliptical confidence limit can be greatly reduced by reducing the variation of the tightening work coefficient. We also experimentally found that the tightening work coefficient was 0.122 as mentioned above, and if the range of working conditions is narrowed, it is possible that the tightening work coefficient a can be considerably reduced.

FIGURE 11 Control of tightening work coefficient

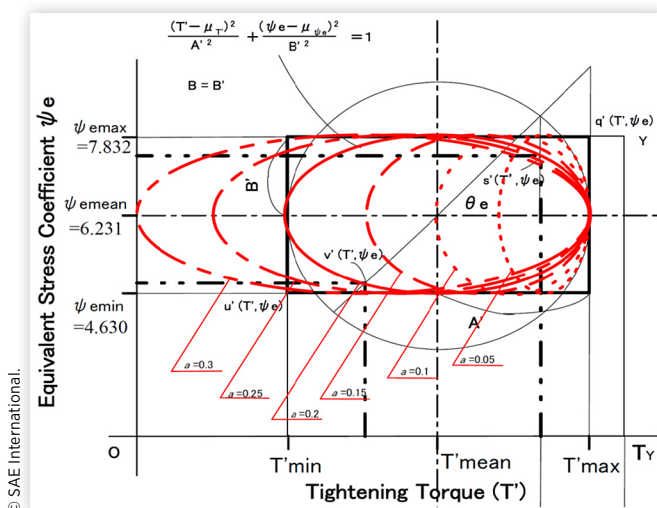


FIGURE 12 Distribution of clamping force and equivalent stress

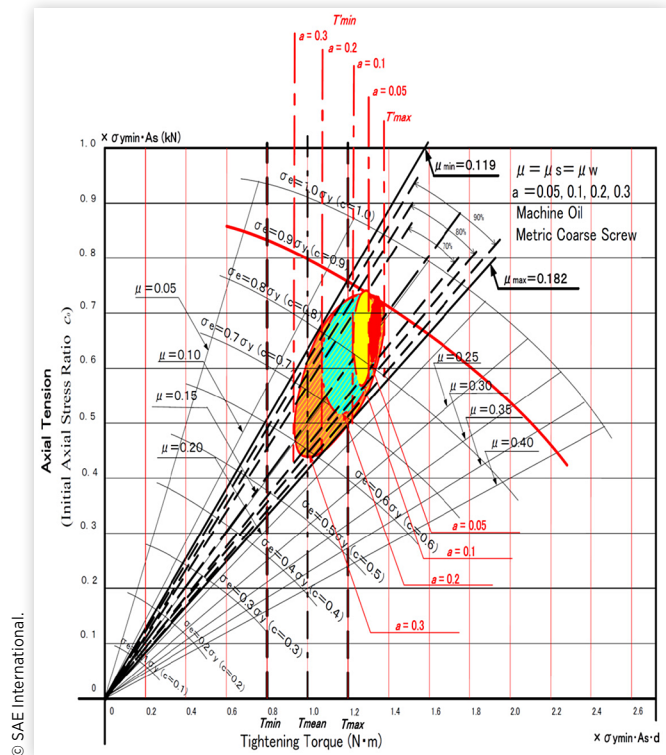


Figure 12 schematically shows the state of the elliptical confidence limit under the following combinations of conditions:

1. $a=0.3, \mu=100\%$,
2. $a=0.2, \mu=90\%$,
3. $a=0.1, \mu=80\%$,
4. $a=0.05, \mu=70\%$.

The dispersion of the coefficient of friction μ can be seen to be small under the same tightening conditions as in the case of obtaining the tightening work coefficient. To determine these conditions, as described in the previous study, tightening tests with various bolts, tools, and lubrication conditions are essential [4].

From the figure, it can be seen that higher tightening torque, higher axial stress, and higher equivalent stress can be obtained with small variation as a result of selecting a suitable value of a , that is, as a result of an approach based on production technology.

Summary/Conclusions

It is important to provide high initial axial tension to ensure tightening reliability and prevent self-loosening and fatigue breakage. In our previous study, the statistical distribution of the magnitude of the combined stress (equivalent stress) was formulated and proposed using shear strain energy theory. In this study, the torque coefficient and equivalent stress

coefficient, which are both affected by the coefficient of friction, were also formulated for a bolted joint tightened by the calibrated wrench method.

The conclusions of this study are as follows.

1. In general, the variations (confidence limit) of clamping force and equivalent stress for a large number of bolted joints tightened at a factory site are conventionally thought to have a rhombic distribution. However, when considering the tightening torque, clamping force, and equivalent stress to be independent random variables, the distribution becomes elliptical.
2. The elliptical confidence limit is inside the rhombic variation, so the variation is smaller. Therefore, the maximum value within the variation has a larger margin to the maximum clamping force (or yield point, etc.) for an elliptical confidence limit than for a rhombic variation.
3. It is valid to consider k and T' and also ψ_e and T' as independent random variables. Then, from the results of theoretical analysis, the relationship between k and T' and also the relationship between ψ_e and T' are expressed as elliptical confidence limits.
4. Using this elliptical confidence limit distribution, we formulated the procedure of analyzing the optimum tightening torque, and the results for a metric coarse screw with different tightening work coefficients are shown in the [appendix](#) as an example of a trial calculation.
5. Under such circumstances, in this study, the conventional viewpoint is expanded and the viewpoints of the elliptical confidence limit and quality and process control are introduced, which should contribute to improving the tightening reliability of bolted joints.

To maintain the tightening reliability of bolted joints, standardization of the tightening work in a production site is very important. We think that this method will be useful for establishing job standards (technical engineering standards).

References

1. Hareyama, S. and Kodama, S., "A Study on Confidence Limit for Two Independent Probability Variables in Engineering Problems (Applications to Limit of Transmitted Torque in Disk Clutch and Bolt Axial Tension Control)," *JSME International Journal (Series III)* 33(2):256-262, 1990.
2. Hareyama, S., Manabe, K., and Nakashima, M., "Improving Tightening Reliability on Bolted Joints for Calibrated Wrench Method (an Analysis on Optimum Tightening Torque by Confidence Limit Ellipse)," in *Proceedings of ASME, 2B: Advanced Manufacturing*, IMECE2013-63387, 2013, 12.
3. Hareyama, S. and Manabe, K., "Advantage of Elliptical Confidence Limit Method for Bolted Joint Tightening Reliability," in *Proceedings of ASME, IMECE2015-50729*, 2015, 10.
4. Hareyama, S., Manabe, K., Shimodaira, T., and Naganawa, T., "Experimental Study to Verify Elliptical Confidence Limit Method for Bolted Joint Tightening," in *Proceedings of ASME*, IMECE2016-66336, 2016, 9.
5. Hareyama, S., Manabe, K., Shimodaira, T., and Hoshi, A., "Working Load Analysis and Strength Estimation for Bolted Joints during Actual Machine Operation," in *Proceedings of ASME*, IMECE2014-39193, 2014, 10.
6. Hareyama, S., Manabe, K., and Kobayashi, S., "Loosening Lifetime and Residual Clamping Force Prediction Method on Bolted Joints and Evaluation Criterion of Clamping Force Level for Prevention of Loosening Failure," SAE Technical Paper 2019-01-1111, 2019, <https://doi.org/10.4271/2019-01-1111>.
7. Bickford, J.H., *An Introduction to the Design and Behavior of Bolted Joints* Third Edition (CRC Press, 1995), 213-268.
8. Nassar, A.S. and Yang, X., "Novel Formulation of the Tightening and Breakaway Torque Components in Threaded Fasteners," *Transactions of ASME, Journal of Pressure Vessel Technology* 129:653-663, 2007.
9. Amir, Y., Govindarajan, S., and Iyyanar, S., "Bolted Joints Modeling Techniques, Analytical, Stochastic and FEA Comparison," in *Proceedings of ASME, IMECE2012-85055*, 2012, 12.
10. Kopfer, H., Friedrich, C., Agostinis, M.D., and Croccolo, D., "Friction Characteristics in Light Weight Design Focusing Bolted Joints," in *Proceedings of the ASME, IMECE2012-85940*, 2012, 8.
11. Bickford, J.H., "Preventing Failure in Bolted Joints Part 1-Avoiding Assembly Errors," *Machine Design* 50(18):100-104, 1978.
12. Kawasaki, K., Takahashi, A., and Asai, M., "The Control of Screw Fastening Torque and a Method for Checking It," *Journal of the Japan Society of Precision Engineering* 42(6):108-113, 1976 (in Japanese).

Contact Information

Mr. Soichi Hareyama, Dr. Eng. Visiting Researcher,
Tokyo Metropolitan University, Japan
hare-lab@ivy.ocn.ne.jp
hareyama-soichi@tmu.ac.jp

Acknowledgments

We would not have been able to perform this research without the previous results of many researchers and engineers, who provided various helpful suggestions. We thank the pioneering researchers from the bottom of our hearts.

